RESEARCH PAPER

ELECTROCHEMICAL POLYMORPHIC PHASE FORMATION IN METALS

Oleg B. Girin[1)]*

[1)] Materials Science Department, Ukrainian State University of Chemical Technology, 8 Gagarin Ave., 49005 Dnipro, Ukraine

* Corresponding author: girin@ua.fm, tel.: +38 056 7535829, Materials Science Department, Ukrainian State University of Chemical Technology, 8 Gagarin Ave, 49005 Dnipro, Ukraine

ABSTRACT

The phenomenon of electrochemical phase formation in metals and alloys via a supercooled liquid state-stage was discussed. Assuming the electrodeposited metal to be a product of formation and ultrarapid solidification of supercooled metallic liquid, a possibility of metastable phase formation during electrodeposition of polymorphous metals was suggested. It was anticipated that the polymorphic transition of the metal's metastable form to the stable one occurs by shear, as does the martensitic transformation. To enable revealing an orientation relationship between grains of the two phases, a method for X-ray texture analysis of metals was developed using a combination of direct pole figures. It was established that the phase formation during electrodeposition of polymorphous metals produces metastable modifications typical of entities that crystallized from a liquid state at extremely high rates. In regards to polymorphic transitions in metal electrodeposition, certain orientation relationships were observed between grains of the stable and the metastable phase, which is typical of phase transformations proceeding at extremely high rates. The results obtained provided additional arguments in favour of the phenomenon under discussion.

Keywords: electrochemical phase formation; electrodeposited metal; liquid state; polymorphic transformation; texture

INTRODUCTION

It is well-known that data on the phase composition, structure, texture and structural defects of the applied layers is extremely necessary to develop advanced technologies for producing electrodeposited coatings having improved physical [1-3], mechanical [4-6] or chemical [7-9] properties. These data can be predictably controlled using the recently established phenomenon of electrochemical phase formation in metals and alloys via a supercooled liquid state-stage [10-14]. The discovered phenomenon occurs during the electrochemical deposition of metals or alloys in an aqueous medium onto a solid cathode when a deeply supercooled metal liquid evolves in the form of a multitude of liquid atomic clusters that appear in an avalanche-like manner at various places near the cathode or the growing deposit and then solidifies ultra-rapidly at the deposition temperature.

This phenomenon is due to an extremely rapid, burst-like liberation of the metal or alloy, resulting from a chain reaction of electrochemical formation of atoms and transition of the atomic clusters or their associations from a liquid to a more stable solid-state [11].

Developing views are fundamentally different from the current concepts, according to which electrochemical phase formation in metals occurs by "incorporation" or "embedding" of ions from the water solution or of atoms (adatoms or adions) evolved at deposit surface into the deposit crystal lattice [15-17]. Despite the lack of satisfactory experimental evidence for the validity of these concepts, they remain the main ones for theoretical discussion of the issues of electrochemical phase formation [18-22]. Furthermore, these concepts have received theoretical development in recent publications on the electrochemical phase formation in metals and alloys [23-27].

The last two years were marked by new experimental results proving the existence of the phenomenon of the electrochemical phase formation in metals and alloys via a supercooled liquid state stage. Relying on the data obtained, it was found that the discussed phenomenon is proved by the following experimental facts:

- (1) electrochemical phase formation in metals resulting in phases with amorphous structure typical of a solidified metallic liquid when crystallization is hindered in the course of deposition [28];

- (2) the formation enhancement of intermetallic compounds involving metallic cathode elements and the electrodepositing metal plus evolvement of additional intermetallics enriched in cathode elements, on replacing a solid cathode with a chemically identical liquid one [29];

- (3) the formation of intermetallics between solid metallic cathode elements and the solvent in the alloy electrodepositing as substitution solid solution, as well as enhancement of these processes accompanied by the development of additional intermetallics enriched in cathode elements on replacing a solid cathode with a chemically identical liquid one [30];

- (4) with alloys electrodepositing as substitution solid solution at a solid metallic cathode, the formation of intermetallics including cathode elements and the alloy solute element building no distinct phase [30];

- (5) on replacing a solid cathode with a chemically identical liquid one, intermetallics formation is enhanced involving metallic cathode elements and the electrodepositing alloy solute, building no distinct phase, plus additional intermetallics enriched in cathode elements emerge [30];

- (6) with alloys electrodepositing as intermetallic compounds at a solid metallic cathode, formation of intermetallics involv-

ing components of the depositing alloy and, in parallel, cathode elements and alloy components is observed [31];
- (7) on replacing a solid cathode with a chemically identical liquid one for alloys electrodepositing as intermetallic compounds, additional intermetallics enriched in the major alloy component and cathode elements are formed [31].

The aim of the work was the further experimental verification of the existence of the phenomenon in point.

PRINCIPAL HYPOTHESIS

It was shown in paper [28] that it is possible to deliberately produce deposits in the amorphous state by targeted action on the liquid phase of the metal as it solidifies in electrodeposition. The amorphous entities synthesized by electrochemical deposition are all metastable and will sooner or later change to stable crystalline structures; it will happen sooner on exposure to external factors.

If the phenomenon in question exists, one can logically assume it possible also to synthesize electrodeposits in some metastable crystalline state that would display phase- and structure-related features typical for metal ultrarapid crystallization from the liquid state.

Among the most frequent types of metastable crystalline structures are polymorphs that are only stable in the higher sections of the metal's crystallization temperature range. Such metastable polymorphs are intermediate products of conversion from metallic liquid to stable crystalline packing and maybe frozen at room temperature by extremely rapid solidification, e. g. by liquid quenching [32, 33].

Targeted synthesis of electrodeposited polymorphous metals in the shape of metastable polymorphs surviving at room temperature may provide another argument for the phenomenon in point.

IDEA OF EXPERIMENT

It is well-known that the metallurgical polymorphous metal if it solidifies slowly, will sequentially form different crystalline polymorphs that are stable in their respective temperature ranges. However, if the solidification is very rapid, one or other of the metal's high-temperature modifications may be quenched and then remain in a metastable state at room temperature for a while, converting to a stable phase with time [32, 33].

Recently it was shown that under slowing down the polymorphic transformation process in the metal being electrodeposited, the texture formation is intensified in the metastable modification, but suppressed in the stable modification [34]. Accordingly, the weighty argument for the phenomenon in point will be electrochemical phase formation in polymorphous metals leading to solely metastable polymorphs typical of metal crystallization from a liquid state at extremely high rates. Another argument is based on the following considerations. If the phenomenon in point exists, then conversion of the frozen metastable polymorph to some other form stable at given thermodynamic conditions may be possible because due to some decrease of solidification rate in electrodeposition. Such diffusionless shear transitions of the martensitic type have extremely rapid rates and do not necessarily lead to the complete disappearance of the initial phase.

For such phase transformation in an electrodeposited metal, one should expect that a two-phase crystalline structure will arise that includes both metastable and stable modification. A specific feature of such transformation will be obedience to a distinct orientation relationship between the two-grain lattices in the initial and the newly formed phase. In other words, the stable modification's grain lattice will be regularly oriented with respect to the grain lattice in the metastable polymorph.

It has been known that the solidification of pyrometallurgical cobalt at very high rates involves a diffusionless polymorphic transformation $\beta \rightarrow \alpha$ occurring by shear (as does martensitic transition) [35]. Further, it was established [36] that the $\beta \rightarrow \alpha$ transformation in cobalt single crystals subjected to quenching from 1000 °C leads to martensitic α-grains' orientations consistent with the Nishiyama-Wassermann relationship: $\langle 11.0 \rangle \alpha \parallel \langle 110 \rangle \beta$.

If the phenomenon in question exists, then the above orientation relationship between the stable and the metastable polymorph must hold for electrodeposited cobalt as well.

MATERIAL AND METHODS

To implement the above idea, a study was carried out into the structure of samples of the polymorphous metal manganese obtained by electrodeposition in ammonium chloride solution at room temperature and current densities ranging from 5.0 to 25.0 A dm^{-2} (at every 5.0 A dm^{-2}). Also studied were electrodeposits of the polymorphous metal cobalt obtained at room temperature and current densities from 5.0 to 20.0 A dm^{-2} (at every 5.0 A dm-2).

X-ray diffraction analysis was carried out using a modified DRON-3 X-ray diffractometer with Cu-Kα irradiation. To measure the orientation distribution of grains of the stable and the metastable polymorphs, Cr-Kα data from a modified DRON-2 X-ray diffractometer were used.

Methodological backing for the idea of the experiment

Since the hcp structure of α-Co is less symmetrical than a cubic arrangement, the X-ray texture analysis of this phase presents some difficulties. With cubic metals having a perfect axial texture, it is sufficient to consider just the central part of the direct pole figure. This is due to the high repeatability of poles for identical lattice planes both in the centre and at the periphery of the stereographic projections. With hexagonal metals that are less symmetrical than cubic ones, any thorough analysis into preferred orientations must involve peripheral areas in addition to the central part of the direct pole figure. In such a case, supplementary X-ray techniques of texture analysis must be employed.

To implement the idea of the experiment, it is thus desirable to develop a simple, reliable and unambiguous technique for the analysis of texture in hexagonal metals. The method offered to identify preferred orientations of grains corresponding to the peripheral part of a direct pole figure involved examination of the central part of a complementary direct pole figure whose indices meet the following condition:

$$h_1 h_2 + k_1 k_2 + l_1 l_2 = 1, \qquad (1.)$$

where: $h_1 k_1 l_1$ - indices of the main direct pole figure
$h_2 k_2 l_2$ - indices of the complementary direct pole figure

The necessity to generate the central part of the complementary direct pole figure that satisfies condition (1) is dictated by the following. In an examination into hcp metal texture using the central part of a direct pole figure, e. g. with indices (00.1), the peripheral part of the figure from 60° to 90° will remain unsolved. The reason is that the lower angular limit of the peripheral part corresponds to the maximum specimen inclination angle in diffractometer around an axis lying in the goniometer equatorial plane.

If an axial texture with an axis perpendicular to plane {10.1}, {20.1}, {10.0}, {11.1}, {11.0} or {21.1} whose poles belong to the above angular range is present in the specimen, it will not be detected by way of analysis of the central part of the direct pole figure (00.1). This is illustrated by the stereographic projection (00.1) for the hexagonal system in Fig. 1a. Its

central part extending from 0° to 60° displays no poles for the above planes. Note that the stereographic projections (00.1) and (10.1) for the hexagonal system with c/a = 1.623 (for α-Co) were not taken from literature but calculated and constructed especially, see **Fig. 1**.

Fig. 1 Stereographic projections (00.1) (a) and (10.1) (b) for the hexagonal system (*c/a* = 1.623)

To reveal possible grain orientations corresponding to the peripheral part of the direct pole figure (00.1), it is necessary to build up the central part of its complementary direct pole figure whose projection axis coincides with the normal to one of the above planes. It was experimentally found that the choice of the complementary direct pole figure is defined by ratio (1).

Accordingly, in the event the central part of the direct pole figure (00.1) is constructed, it is necessary to construct the central part of one or other of the following direct pole figures: (10.1), (20.1), (21.1) or (11.1) so that the preferred orientations of grains corresponding to the peripheral part of the figure can be found. An analysis of the central part of any of such direct pole figures will give a full picture of the texture of the peripheral part of the direct pole figure (00.1).

The reason is that the central parts of the stereographic projection (11.1), (21.1), (20.1) or (10.1) (Fig. 1b) include the poles for the planes corresponding to the periphery of the stereographic projection (00.1). However, if the central part of any of the direct pole figures (10.1), (20.1), (21.1) or (11.1) was constructed first, then further analysis of the texture calls for the central part of the direct pole figure (00.1) to be plotted, as required by (1).

Similarly, if the central part of the direct pole figure (10.0) was constructed, there is a need additionally to build the central part of one of the direct pole figures (10.5), (10.4), (10.3) or (10.2) whose indices comply with condition (1). After that, conclusions can be made on the metal texture and degree of its perfection based on a combination of the central parts of the main and the complementary direct pole figure.

If $h_1h_2 + k_1k_2 + l_1l_2 = 0$ or 2, then the accuracy of X-ray texture analysis is impaired owing to duplication of stereographic projections for the same poles of the planes over the angular range from 30° to 60°. The accuracy of orientation identification gets worse with growing distance from the centre of the direct pole figure because of X-ray beam spreading, defocusing arising from specimen inclination etc. Consequently, poorer accuracy for any of the two direct pole figures is to be expected for the grain orientations with axes coinciding with the normals to the planes whose poles belong to the above angular range.

The combined direct pole figures method of metal texture analysis, if used to implement the idea of the experiment, will yield exact and reliable information on interrelations between the grain orientations of α- and β-form in electrodeposited cobalt.

RESULTS AND DISCUSSION

Identification of metastable modifications

At room temperature, manganese should exist in a stable bcc form α-Mn as given in reference literature [37]. A unit cell in its complex lattice has 58 atoms compared to just 2 atoms in the case of an ordinary bcc lattice.

The X-ray diffraction studies revealed that manganese electrodeposited at room temperature appears as γ-Mn, a face-centred tetragonal form. **Fig. 2** shows clearly that the diffraction peaks for manganese obtained at room temperature and current density 10.0 A dm^{-2} correspond to γ-Mn. A comparison between the experimental and handbook data on this metastable form indicates a fairly good correlation which substantiates that the manganese electrodeposited as γ-Mn, see **Table 1**.

Fig. 2 Diffraction pattern for manganese electrodeposit illustrating occurrence of metastable γ-Mn form due to ultrarapid solidification of a liquid phase of manganese during electrodeposition

Table 1 Experimental and handbook values of diffraction characteristics for the metastable γ-Mn form in electrodeposited manganese

HKL	Experimental values		Handbook values	
	d/n, nm	I, pps	d/n, nm	I, rel. units
111	0.2130	216	0.2130	1.00
200	0.1895	11	0.1895	0.07
002	0.1761	24	0.1763	0.50
202	0.1289	15	0.1290	0.15
311	0.1133	6	0.1133	0.10
222	0.1064	8	0.1066	0.10

According to [37], the metastable γ-form of manganese is stable in the temperature range from 1358 to 1408 K. The observation of this high-temperature modification in electrodeposits prepared at room temperature testifies to an extremely rapid solidification of the metal liquid phase in electrodeposition.

This finding agrees well with literature data [38, 39] that cite the metastable γ-form as typical of electrodeposited manganese. Also, it is noted in [38] that transition of the metastable γ-

Mn to a stable α-Mn form sets on very soon after the completion of electrodeposition. It can thus be concluded that the occurrence of manganese as the metastable γ-modification in electrodeposition is another proof of the phenomenon in point.

In another embodiment of the above idea, structural characterization of the next polymorphous metal was carried out, namely, cobalt obtained by electrodeposition at room temperature. As stated in the literature [37], cobalt should exist in the hcp form α-Co at room temperature.

The diffraction studies revealed electrodeposited cobalt in a metastable fcc form β-Co in the specimens. As is seen in **Fig. 3**, the diffraction pattern for the cobalt obtained at room temperature and current density 15.0 A dm^{-2} point to precisely that metastable modification. **Table 2** confirms that the electrodeposited cobalt appears in the β-form.
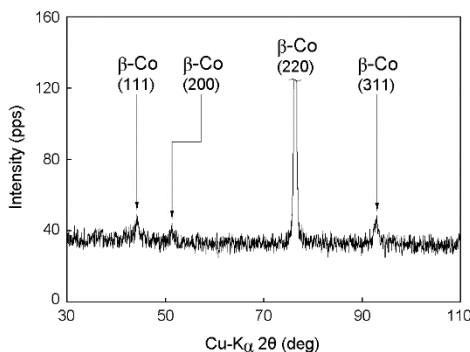
Fig. 3 Diffraction pattern for cobalt deposit indicating occurrence of metastable polymorph β-Co due to ultrarapid solidification of some liquid phase during electrodeposition

The stability range for this metastable modification stretches between 700 and 1768 K [37]. That cobalt forms the metastable β-phase in electrodeposition at room temperature is an indication of an extremely rapid crystallization rate. The occurrence of this β-form in cobalt deposits prepared electrochemically is confirmed by the literature [40-44].

Table 2 Experimental and handbook values of diffraction characteristics for the metastable modification β-Co in electrodeposited cobalt

HKL	Experimental values		Handbook values	
	d/n, nm	I, pps	d/n, nm	I, rel. units
111	0.2040	50	0.2040	1.00
200	0.1770	45	0.1770	0.44
220	0.1251	196	0.1253	0.22
311	0.1065	53	0.1066	0.22

Consequently, the existence of the metastable β-form (typical of extremely rapid crystallization from a liquid state) in the cobalt prepared by electrodeposition is another proof of the phenomenon in point.

Metastable modification features

The major features of the metastable phases γ-Mn and β-Co formed in electrodeposition are their fine-grained structure [34] and, more importantly, grain orientation. Among other things, differences in the distribution of diffraction peak intensities between the experimental specimens and the handbook data may be an indication of texture formation in the metastable β-modification of the electrodeposited cobalt, see **Table 2**.

According to the handbook data on non-textured specimens, the peak intensity should be at its highest level with (111) β-Co while (220) β-Co peak intensity should be only 0.22 of that value (Table 2). As for the experimental specimens, the relative intensity of (111) β-Co attained a mere 0.26 of the (220) β-Co value taken to be unity. This information suggests that an axial texture with an axis [110] possibly arose in the cobalt specimen at hand.

To check this suggestion, X-ray texture analysis was carried out for the β-Co synthesized. It was found that its texture included an axial orientation with an axis [110] and a random component, see **Fig. 4**.

Fig. 4 Texture-relevant curve of interference by {111} (a) and direct pole figure (111) (b) for electrodeposited cobalt: 1 and 2 – respective texture recordings for the experimental and the reference specimen, 3 – background line, 4 to 8 – iso intensity levels for diffracted X-rays

This result made a basis for further experiments to prove the existence of the phenomenon in point. Indeed, if the metastable form in the electrodeposited metal has a preferred orientation, the stable modification in the metal likewise will have one, owing to the very high phase transformation rates. Moreover, there must be a clearly defined orientation relationship between the grains of the metastable and the stable form in the electrodeposited polymorphous metal.

Obedience to distinct orientation relationship between the grains of stable and metastable form in electrodeposited polymorphous metal.

In order to clarify the interrelationship between the lattices of the α- and β-forms in electrodeposited cobalt, an X-ray texture examination was carried out on two-phase cobalt deposits. The specimens were obtained by electrodeposition in a sulphate solution at room temperature and a current density of 5.0 A/dm².

The texture examination of the hcp α-Co involved the suggested method that combined direct pole figures (10.1) and (10.0) while the fcc β-Co was examined by the use of a direct pole figure (111). To do this, texture curves for interference on {10.1} and {10.0} of the α-Co were recorded and subsequently used to construct direct pole figures (10.1) and (10.0) for the α-modification, see **Fig. 5**.
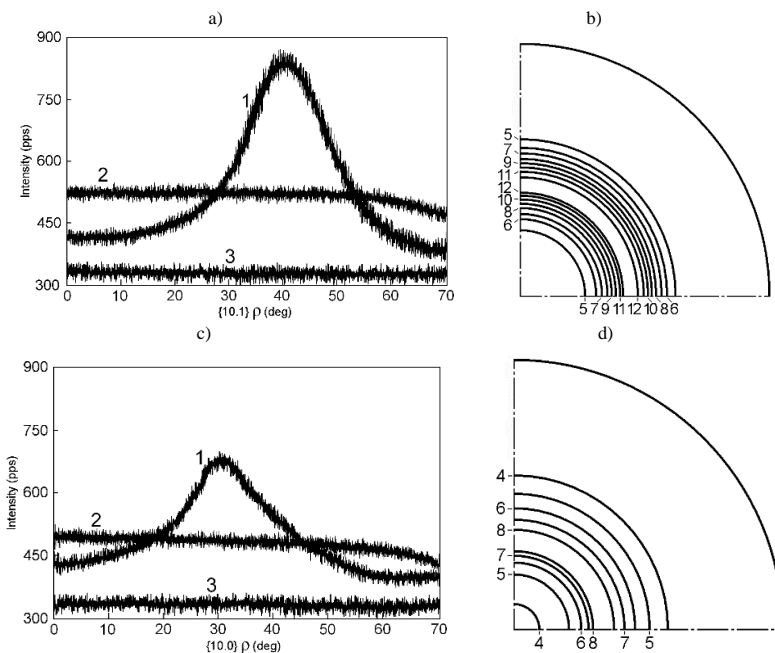
Fig. 5 Texture-relevant curves of interference by {10.1} (a) and {10.0} (c) for α-modification in two-phase cobalt electrodeposit and their respective direct pole figures (10.1) (b) and (10.0) (d): 1 and 2 – texture curve records for specimen and reference piece respectively; 3 – background line; 4 to 12 – iso intensity levels for diffracted X-rays

The direct pole figure (111) for the β-modification of cobalt in **Fig. 6** was constructed from the experimental texture curve of interference by {111} in β-Co. These experiments showed that the α-phase texture in a two-phase specimen of electrodeposited cobalt is represented by an axial orientation with an axis [11.0] normal to the specimen surface. This conclusion was made based on the presence of a texture peak for the axial orientation [11.0] at an angle of 40.1° in the pole figure (10.1) for the α-modification (Fig. 5c), in combination with the texture peak of the same orientation of grains at 30.0° in the pole figure (10.0) for this phase, see Fig. 5d.
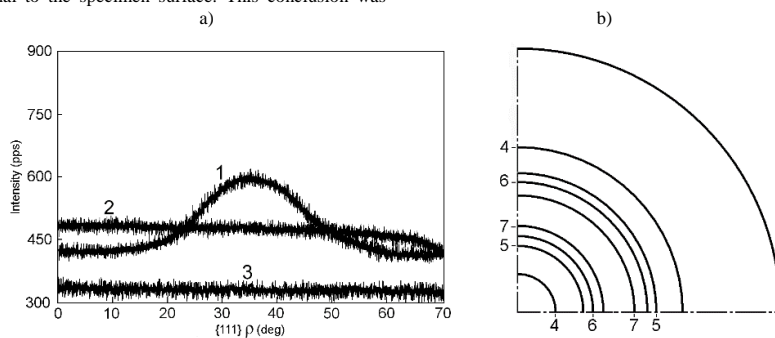

Fig. 6 Texture-relevant curve of interference by {111} (a) and direct pole figure (111) (b) for β-modification in two-phase cobalt electrodeposit: 1 and 2 – texture curve records for specimen and reference piece respectively; 3 – background line; 4 to 7 – iso intensity levels for diffracted X-rays

For the β-modification in the same specimen, the X-ray texture analysis revealed that its axial texture is represented by an axis [110] normal to its surface. This conclusion was made considering the texture peak of axial orientation with the axis [110] at an angle of 35.3° in the pole figure (111) for the β-phase in the two-phase cobalt specimen (Fig. 6b).

In all, it was found that the texture of a two-phase electrodeposited cobalt specimen included the axial orientations with the axes [11.0] in the α-Co and [110] in the β-Co, both normal to the specimen surface and combined with a random component. Since both the axis [11.0] of α-Co and the [110] of β-Co is normal to the specimen surface, they must be parallel to one another. Hence, a distinct orientation relationship exists between the lattices of the two phases α and β in electrodeposited cobalt, namely $\langle 11.0 \rangle_\alpha \parallel \langle 110 \rangle_\beta$.

An identical orientation relationship was found for pyrometallurgical cobalt in which the polymorphic transition β→α occurred by shear, i. e. was of martensitic type [36]. It may be therefore concluded that the phase transition from metastable to a stable form of a polymorphous metal in electrodeposition involves a shear mechanism, which is due to extremely high rates of crystallization.

Mechanism of metastable-to-stable phase transition in the electrodeposition of a polymorphous metal

In what follows, a concept is offered for the transition of the metastable β-Co to the stable α-Co in the course of ultrarapid solidification in the electrodeposition of cobalt. The fcc and hcp lattices of the respective modifications are similar in packing index (0.74), coordination number (12) and ordering of the closely packed planes {111} and {00.1} along which the atoms move. For this reason, an fcc to hcp transition with retention of the orientation relationship as established here is possible by a cooperative directed displacement of atoms to less-than-interatomic distances not involving atomic position exchange.

Since the lattices of the stable and the metastable polymorph are coherent, the continuous change of the metastable to the stable lattice as grains of the stable phase grow is extremely rapid even at room temperature. The reason is that such transition does not require diffusion involving atoms travelling to greater-than-interatomic distances.

As grains of the stable modification grows, elastic stresses build up in the coherent interface region due to the specific volume difference between the stable and the metastable phase. When the proportionality limit is exceeded, the coherence of the lattices is broken, so the stresses are reduced and an interface with a disordered atomic arrangement arises between the two phases.

The lattice conjugation is also disrupted when grain or subgrain boundaries or other lattice defects in the metastable phase are reached by a growing grain. A disruption of lattice coherence makes cooperative displacement of atoms no longer possible and a two-phase structure gets frozen in the deposit.

The proposed shear mechanism of metastable to stable transition in metal electrodeposition is confirmed by experimental data [45]. That study dealt with phase change features as the epitaxial cobalt film thickness grows in the course of electrochemical deposition. An fcc to hcp transition was observed in the thin cobalt films having a [110] orientation as they reached a certain thickness. The transition was quite prompt and was accompanied by a reduction in stresses that had built up in the film [45].

Even though the metastable to stable transition in the electrodeposition of a polymorphous metal occurs by shear, one should bear in mind that phase and/or structure change by diffusion may take place after the electrolysis completion.

In all, one more argument for the phenomenon in point has been obtained, namely a distinct orientation relationship between grains of stable and metastable modification in electrodeposited polymorphous metal, a typical feature of extremely rapid phase transitions.

CONCLUSION

Assuming the electrodeposited metal to be a product of formation and ultrarapid solidification of supercooled metallic liquid, a possibility of metastable phase formation during electrodeposition of polymorphous metals was suggested. This suggestion was based on the knowledge that metastable phase freezing may occur in the course of extremely rapid crystallization involved in casting a polymorphous metal, e.g. by liquid quenching.

Furthermore, it was anticipated that the polymorphic transition of the metal's metastable form to the stable one occurs by shear, as does the martensitic transformation. A marker of this transformation type is adherence to a distinct orientation relationship between grains of the stable and the metastable form.

To enable revealing an orientation relationship between grains of the two phases, a method for X-ray texture analysis of metals was developed using a combination of direct pole figures.

It was established that the phase formation during electrodeposition of polymorphous metals produces metastable modifications typical of entities that crystallized from a liquid state at extremely high rates. In regards to polymorphic transitions in metal electrodeposition, certain orientation relationships were observed between grains of the stable and the metastable phase, which is typical of phase transformations proceeding at extremely high rates.

The results obtained provided additional arguments in favour of the phenomenon under discussion.

REFERENCES

1. E. Yoo et al.: J. Alloys Compd., 843, 2020, 155902. https://doi.org/10.1016/j.jallcom.2020.155902.

2. F. Guo, X. Yu, M. Wang: J. Electrochem. Soc., 167, 2020, 063506. https://doi.org/10.1149/1945-7111/ab8648.

3. H. D. Merchant, O. B. Girin: Defect Structure and Crystallographic Texture of Polycrystalline Electrodeposits, Proceedings of the Materials Research Society Symposium, *Electrochemical Synthesis and Modification of Materials*, edited by P.C. Andricacos, Pittsburgh, USA, Vol. 451, 1997, p. 433-444. https://doi.org/10.1557/PROC-451-433.

4. S. Zhang, S. Kobayashi: J. Mater. Sci., 55, 2020, 5627-5638. https://doi.org/10.1007/s10853-020-04378-z.

5. T. L. Tepla, I. V. Izonin, Z. A. Duriagina, R. O. Tkachenko: Arch. Mater. Sci. Eng., 1(93), 2018, 32-40. http://dx.doi.org/10.5604/01.3001.0012.6944.

6. R. A. Shakoor et al.: Coatings, 7(10), 2017, 161-169. http://dx.doi.org/10.3390/coatings7100161.

7. F. I. Danilov, O. B. Girin, E. R. Popov: Zashchita Metallov, 29(6), 1993, 942-944. https://inis.iaea.org/search/search.aspx?orig_q=RN:26036573

8. O. B. Girin: Mater. Sci. Forum, 561-565, 2007, 2369-2372. https://doi.org/10.4028/www.scientific.net/MSF.561-565.2369

9. U. K. Sultana, A. P. O'Mullane: ACS Appl. Energy Mater., 1(6), 2018, 2849-2858. https://doi.org/10.1021/acsaem.8b00489.

10. O. B. Girin, G. M. Vorob'ev: Russian metallurgy. Metally, 4, 1987, 148-152.

11. O. B. Girin, V. P. Khlyntsev: Elektronnaya Obrabotka Materialov, 3, 2000, 13-18.

12. O. B. Girin: Surf. Eng. Appl. Electrochem., 53(2), 2017, 137-143. https://doi.org/10.3103/S1068375517020041.

13. O. B. Girin: Surf. Eng. Appl. Electrochem., 53(3), 2017, 233-239. https://doi.org/10.3103/S1068375517030048.

14. O. B. Girin: Surf. Eng. Appl. Electrochem., 53(4), 2017, 339-344. https://doi.org/10.3103/S1068375517040056.

15. A. Milchev: *Electrocrystallization. Fundamentals of Nucleation and Growth*, New York: Kluwer Academic Publishers, 2002.

16. E. B. Budevski, G. T. Staikov, W. J. Lorenz: *Electrochemical Phase Formation and Growth: An Introduction to the Initial Stages of Metal Deposition*, Weinheim: WILEY-VCH Verlag Gmbh, 2008.

17. Yu. D. Gamburg, G. Zangari: *Theory and Practice of Metal Electrodeposition*, New York: Springer Science, 2011.

18. J. Chen, S. Luo, Y. Liu, S. Chen: ACS Appl. Mater. Interfaces, 8(31), 2016, 20448-20458. https://doi.org/10.1021/acsami.6b04545.

19. P. Altimari, F. Pagnanelli: Electrochim. Acta, 205, 2016, 113-117. https://doi.org/10.1016/j.electacta.2016.04.093.

20. P. Altimari, F. Pagnanelli: Electrochim. Acta, 206, 2016, 116-126. https://doi.org/10.1016/j.electacta.2016.04.094.

21. V. A. Isaev, O. V. Grishenkova: J. Solid State Electrochem., 18(9), 2014, 2383-2386. https://doi.org/10.1007/s10008-014-2489-9.

22. J. Torrent-Burgues: J. Solid State Electrochem., 17(2), 2013, 373-378. https://doi.org/10.1007/s10008-012-1872-7.

23. X. Zhou, Y. Wang, Z. Liang, H. Jin: Materials, 11(7), 2018, 1124-1132. https://doi.org/10.3390/ma11071124

24. M. Romero-Romo et al.: J. Electroanal. Chem., 791, 2017, 1-7. https://doi.org/10.1016/j.jelechem.2017.03.003

25. E. Mladenova, A. Milchev: J. Solid State Electrochem., 21(6), 2017, 1599-1604. https://doi.org/10.1007/s10008-017-3511-9.

26. A. Milchev: Nanoscale, 8(29), 2016, 13867-13872. https://doi.org/10.1039/C6NR02354A.

27. G. Staikov: Nanoscale, 8(29), 2016, 13880-13892. https://doi.org/10.1039/C6NR01547F.

28. O. B. Girin: J. Chem. Technol. Metall., 54(2), 2019, 391-396. https://dl.uctm.edu/journal/node/j2019-2/18_18-74_p391%20-%20396.pdf.

29. O. B. Girin, D. G. Korolyanchuk: Surf. Eng. Appl. Electrochem., 56(1), 2020, 28-40. https://doi.org/10.3103/S1068375520010068.

30. O. B. Girin, D. G. Korolyanchuk: Surf. Eng. Appl. Electrochem., 56(3), 2020, 289-300. https://doi.org/10.3103/S1068375520030059

31. O. B. Girin, D. G. Korolyanchuk: Surf. Eng. Appl. Electrochem., 56(4), 2020, 501-509. https://doi.org/10.3103/S1068375520040067.

32. I. S. Miroshnichenko: *Quenching from a Liquid State*, Moscow: Metallurgy, 1982.

33. A. M. Glezer, I. E. Permyakova: *Melt-Quenched Nanocrystals*, Boca Raton: CRC Press, 2013.

34. O. B. Girin, V. I. Ovcharenko, D.G. Korolyanchuk: Acta Metall. Slovaca, 25(4), 2019, 267-275. http://dx.doi.org/10.12776/ams.v25i4.1357.

35. B. I. Nikolin: *Multilayer and Polytypical Structures in Metallic Alloys*, Kiev: Naukova dumka, 1984.

36. Yu. V. Khlebnikova, T. I. Tabatchikova, D. P. Rodionov, V. A. Sazonova: Bull. Russ. Acad. Sci. Phys., 73(9), 2009, 1207. https://doi.org/10.3103/S106287380909007X.

37. M. Bauccio: *ASM Metals Reference Book*, 3rd ed., Materials Park: ASM International, 1997.

38. A. V. Vorozhko, I. V. Gamali: Ukrainian Chemical Journal, 39(4), 1973, 392-393.

39. J. Gong, G. Zangari: J. Electrochem. Soc., 149, 4, 2002, C209-C217. https://doi.org/10.1149/1.1452117.

40. A. Vicenzo, P. L. Cavallotti: Electrochim. Acta, 49(24), 2004, 4079-4089. https://doi.org/10.1016/j.electacta.2004.04.001.

41. L. H. Mendoza-Huizar, C. H. Rios-Reyes: Cent. Eur. J. Chem., 11(8), 2013, 1381-1392. https://doi.org/10.2478/s11532-013-0269-5.

42. D. Kaur, D. K. Pandya: J. Electrochem. Soc., 163(6), 2016, D221-D229. https://doi.org/10.1149/2.0311606jes.

43. M. Palomar-Pardavé et al.: Electrochim. Acta, 241, 2017, 162-169. https://doi.org/10.1016/j.electacta.2017.04.126.

44. D. Kong, Zh. Zheng, F. Meng, N. Li, D. Li: J. Electrochem. Soc., 165(16), 2018, D783-D789. https://doi.org/10.1149/2.0191816jes.

45. J. G. Wright: Thin Solid Films, 22(2), 1974, 197-201. https://doi.org/10.1016/0040-6090(74)90006-6.